

## GFUN: AN INTERACTIVE PROGRAM AS AN AID TO MAGNET DESIGN

M J Newman, C W Trowbridge, L R Turner\*  
Rutherford High Energy Laboratory  
Chilton, Didcot, Berkshire, England

### Abstract

A new package of programs, called GFUN, has been developed for designing and calculating the fields of two-dimensional and three-dimensional magnets. The field due to the magnetisation of the iron is calculated directly. "DRAW" subprograms simplify the input of data for the iron and current regions, and display a picture of the iron and current elements for checking as they are read in. "GETB" subprograms allow the field at a point, along a line or over a region to be typed, graphed or contoured. Automatic optimisation is provided. GFUN results have been checked against TRIM calculations and against the measured fields of existing magnets. GFUN is being used for several magnets currently being designed at the Rutherford Laboratory.

### 1. Introduction

Over the past two years we have developed at the Rutherford Laboratory a magnet design package called GFUN. We used three criteria in deciding how to develop it.

1. It should be easy for the magnet designer to use. Most of the work of data input should be done by the computer. The input data should be displayed for checking. Results should be displayed in a way to make interpretation simpler.
2. It should be interactive. Calculating interactively saves the magnet designer time. His train of thought is not broken as it is when he must submit a job and wait minutes or days for the results. His ideas or doubts can be checked immediately. For example he can see from the picture if he has set up the problem incorrectly or awkwardly, or he can follow up anything interesting the graph of the field reveals. He can stop when a line of thought proves unprofitable, and he need not provide in advance for all possibilities. For these reasons GFUN has been designed as an interactive package. However on-line facilities are not always available, and much of GFUN can be used in an off-line mode.
3. It should be available in both two-dimensional and three-dimensional versions, which the user operates with similar commands. This criterion led to the choice of a direct calculation approach. The difficulties of a general mesh generator in three dimensions and the resulting enormous set

of finite difference equations seemed a daunting task. The finite element approach, which also leads to a very large number of equations, was more attractive from the data generator aspect, but had not yet been developed sufficiently. The fact that only the iron regions need to be divided into elements and produce equations to be solved seemed a definite advantage of the direct method. Our experience to date supports our choice.

Even in two dimensions, direct calculation of magnetisation fields is more convenient for the magnet designer than finite-difference or finite-element methods. With those methods, the boundary value of the field or potential must be prescribed. In practice the boundaries must be located far from the magnet, and the field must be calculated over this external region, which may be of no interest to the designer. Even worse, the whole system - conductor, iron and free space - must be spanned by a mesh, which has to be as complex as the most complex part of the system. With a direct-calculation method, on the other hand, only the iron region need be divided into elements. There are far fewer elements; and, however complex the current geometry, the mesh of iron elements can take advantage of the simplicity of the iron geometry.

### II. Hardware and Software

GFUN is used with the IBM360/195 at the Rutherford Laboratory. Although the central computer has two megabytes of core storage, only 160 kilobytes are available for an on-line program, and GFUN operates in that. Two peripherals are used; a typewriter for input and output of text and a Computek 400/15 Storage Tube Display for output of pictures and text.

A satellite computer (Honeywell DDP224) handles messages between these peripherals and the GFUN program in the central computer. Locally written software in the 360/195 communicates with routines in the supervisor program, which manages all on-line input and output. The overall system is known as DAEDALUS<sup>2</sup>. Further software packages<sup>3,4</sup> in GFUN prepare the graphical output and diagnose errors in messages from the typewriter.

### III. The Direct Calculation Method

#### Background

In contrast to the partial differential equation method the integral equation or direct-method has not been used extensively in the solution of the magnetostatic problem. The

---

\* Present address: Physics Department,  
Muskingum College, New Concord, Ohio.

preliminary work of A Halacsy<sup>5</sup> at the University of Nevada, USA, in the dipole formulation is well known and the series of computer programs RENO 1, RENO 2 and RENO 3 apply the direct solution method to the solution of the magnet problem. A formulation in terms of vector potential for an assembly of dipoles was described by S Sackett<sup>6</sup> of LRL and a passing reference was given to a program called TAMI based on the method. Recently there has appeared several papers from a group at Toronto University, Canada, giving detailed analysis of the different formulations of the integral equation method. Notably Zaky<sup>7</sup> and Robertson<sup>8</sup> who described several mathematical models and gave results for some linear problems.

Our approach has followed similar lines in as much as we have used the magnetic field intensity vector formulation but our method of discretisation is to replace the iron regions by a number of arbitrarily shaped elements and to treat the magnetisation as constant throughout each element.

#### How it Works

In GFUN  $H_c$ , the field due to the currents and  $H_m$  the field due to the magnetisation of the iron, are each found directly and added to give the total field:

$$H = H_c + H_m \quad (1)$$

In the usual magnet design situation, in which the currents are specified, the field  $H_c$  can be calculated at any point by integrating over the volume of the conductors. In two dimensions, the calculation is analytic and in GFUN is carried out using the techniques described by Beth.<sup>9</sup>

The field  $H_m$  can be written in terms of the scalar potential:

$$H_m = -\text{grad } V_m \quad (2)$$

with the scalar potential written as a volume integral of the magnetisation over the iron region. In SI units,

$$V_m = \frac{1}{4\pi} \int \frac{M \cdot r}{r^3} dV \quad (3)$$

If we: (a) Divide the iron region into  $N$  elements and treat the magnetisation as constant over each;

(b) Take the gradient of Eq (3); and

(c) Integrate over  $z$  to make the equation two-dimensional,

we obtain the following equation for the field at the centre of element  $k$  due to the magnetisation of all the elements:

$$H_{mk} = \sum_{\ell=1}^N C_{k\ell} M_{\ell} \quad (4)$$

where each  $C$  factor depends only on the geometry of the field point and source element.

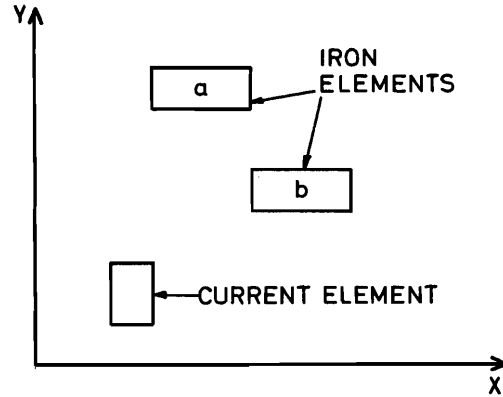


Fig. 1. Geometry of the simply example used to describe the direct method.

For simplicity, let us consider the case in which there are only one current element and two iron elements, as shown in Fig. 1. From Eq (1) and (4), the field at the centre of each element is given by

$$H_a = H_{ca} + C_{aa} M_a + C_{ab} M_b \quad (5)$$

$$H_b = H_{cb} + C_{ba} M_a + C_{bb} M_b$$

But the magnetisation  $M$  can be expressed in terms of the magnetic susceptibility  $\chi$

$$M = \chi H$$

so that

$$H_a = H_{ca} + C_{aa} \chi_a H_a + C_{ab} \chi_b H_b$$

$$H_b = H_{cb} + C_{ba} \chi_a H_a + C_{bb} \chi_b H_b$$

which can be rearranged to read

$$(C_{aa} \chi_a - 1) H_a + C_{ab} \chi_b H_b = -H_{ca} \quad (6)$$

$$C_{ba} \chi_a H_a + (C_{bb} \chi_b - 1) H_b = -H_{cb}$$

Each of the equations in Eq (4) through Eq (6) is a two-component vector equation; each  $C$  is a two by two tensor.

If we knew the susceptibilities  $\chi_a$  and  $\chi_b$ , Eq (6) would be four simultaneous linear equations which could be solved immediately for  $H_a$  and  $H_b$ . Instead we must choose initial values for the

susceptibilities, solve for the fields at the centres of the elements, find the values of susceptibilities corresponding to these fields from the table of known values for the material, and repeat. Depending upon the saturation of the iron, and the number of elements, convergence to a few gauss out of several kilogauss requires twenty to one-hundred iterations.

Then the magnetisation can be determined from the converged values of H and can be stored. Thereafter the field at any point can be found from the stored magnetisation and the appropriate computed C coefficient.

If the magnet being calculated has a plane of symmetry, then only half the current and iron elements need enter the calculation. Likewise, if it has two planes of symmetry, the calculation need include only the elements in one quadrant. The C coefficients are calculated for both the direct and reflected positions of the elements, and the results added or subtracted depending on whether the magnetisation component of the reflected element has the same or opposite sign as the component of the direct element.

#### IV. How the GFUN Package is Used

##### Data Preparation

To begin a new problem in GFUN we might specify the B-H curve of the iron and the symmetry the magnet is to exhibit, eg. no symmetry, dipole, quadrupole, or axial symmetry. Next the iron and current regions are specified. An advantage of the GFUN package is that new shapes of elements and arrays of elements can be added to the "DRAW" sub-program without requiring extensive re-programming of subsequent sub-programs. Shapes that have proved useful are: triangles, rectangles, arrays of triangles or rectangles, and annular sectors or quadrilateral regions mapped by triangles. Examples can be seen in Figure 4. For current elements, the current density or total current density or total current are also specified. Elements can be deleted, replaced, rotated or translated; and after each change they are drawn on the screen for checking.

##### Calculation

The GETM subprograms calculate the magnetisation of the iron elements, as described above. After each iteration the greatest change in field in an element is displayed, until convergence is reached. All data on the problem can at any stage be stored on a disk data set, then read back later and calculations resumed.

Finding the magnetisation of an iron array of N elements requires repeatedly solving a set of 2N equations and thus storing a 2N by 2N matrix. For more than 32 elements, calculation of the magnetisation is done off line. In three dimensional problems, in which 3N equations must be solved and in addition more elements are usually needed, the magnetisation calculation is always done off-line.

#### Display of Results

Once the magnetisation is known, the field at any point can be found immediately. The field due to the current is calculated directly, and the field due to the iron is evaluated by Eq (4) with the C coefficients calculated for each source element and the specified field point.

The GETB subprograms permit the field at any specified point to be typed out, but also permit several optional graphical displays of the field. The variations of the total field, any component of field, or its homogeneity along any horizontal or vertical line can be computed, and its graph displayed. See, for example, Fig. 2, 3, and 8. Also contours of equal strength can be drawn over a region, for total field or any component. This option is of obvious value in judging the homogeneity of the field in its useful region, but is also useful in finding where the highest field occurs in a superconducting coil. See for example Fig. 9 and 10.

#### V. Optimisation

It was decided at the outset that we should include both automatic and manual optimisation in the GFUN program. So far we have concentrated upon the problem of determining conductor shapes to achieve high homogeneity. However the system is capable of generalisation so that any reasonable function of the magnetic field can be minimised over a defined region. The command OPTI is used for optimisation. The user specifies an elliptical region over which the field has to be uniform and the parameter of the conductor he wishes to vary. Thus, for example, if the conducting elements are set at right angles all the x coordinates of the bottom left hand corner may be varied to find the optimum positions. Alternatively the positions may be fixed and the length of the rectangles varied to determine the optimum size. The upper and lower limits may also be specified to prevent overlapping and non-practical cases.

The program chooses suitably spaced points within the elliptical region and constructs a function by forming the sum of squares of the quantity  $\frac{\Delta B}{B_0}$  where  $\Delta B$  is the difference of the field at the point and at the centre of the region, and B is the value of the field at the centre of the region. The function is minimised by use of an algorithm designed by Powell.<sup>10</sup>

##### Example: Design of a Superconducting Dipole

Suppose we want to design a superconducting dipole magnet, with a specified cylindrical iron yoke and a specified useful area over which we want to optimise the field uniformity. We could start with four current regions, set up and drawn by the DRAW subprogram as shown in Fig. 2. Homogeneity along the x axis, calculated and plotted by the GETB subprogram, is seen in Fig. 2 to be poor. Figure 2, and in fact all the figures

except Fig. 1 are hard copies of the screen.

Optimisation by the OPTI subprograms results in the conductor geometry shown in Fig. 3, with a homogeneity of better than one part in  $10^4$ .

Next the iron yoke is put in, divided into 32 elements, again by the DRAW subprograms; see Fig. 4. The GETM subprograms solve for the field and magnetisation in each iron element. Fig. 5 shows how the field converges in 60 iterations. But as Fig. 6 shows, the total field now has more than one per cent inhomogeneity. So the current is re-optimised, and the magnetisation recalculated. Because the change in magnetisation is fairly small, convergence this time requires only a few iterations. Figure 7 now shows a homogeneity of one-half per cent, and repeating the process yields 0.2, 0.09 and 0.04 per cent in subsequent steps.

This design of a superconductor dipole magnet with field homogeneity of 0.04 per cent was carried out in a single on-line session. Figure 8 shows the field homogeneity in both the x and y directions. Figure 9 shows a contour plot of homogeneity over the useful region and Figure 10 a contour plot of total field in the windings to reveal the point at which the field is maximum.

#### VI. Extension to Three Dimensions

The principal changes in going from GFUN as described in the above sections to a three-dimensional version are:

1. In general the fields due to currents cannot be found analytically as they can in two dimensions.
2. There are nine, rather than four, C coefficients between any two elements, and the coefficients are more complicated.
3. Consequently there are three equations per iron element to be solved rather than two.
4. Usually more elements are needed to give a satisfactory solution.
5. The geometry of the current and iron elements is not completely specified by one picture on the screen.

The first point is met by numerical integration, and merely adds length to the program. For example, combinations of iron and current elements in which the field from the currents is axisymmetric and the field from the iron has either two or three planes of symmetry, can be used for C magnets, picture-frame magnets, or pot magnets with non-axisymmetric return paths.

The second, third and fourth points result in a larger number of equations to solve, requiring more time and space. At present the iron elements must be triangular or rectangular prisms, because the C coefficients have not yet been found for other shapes.

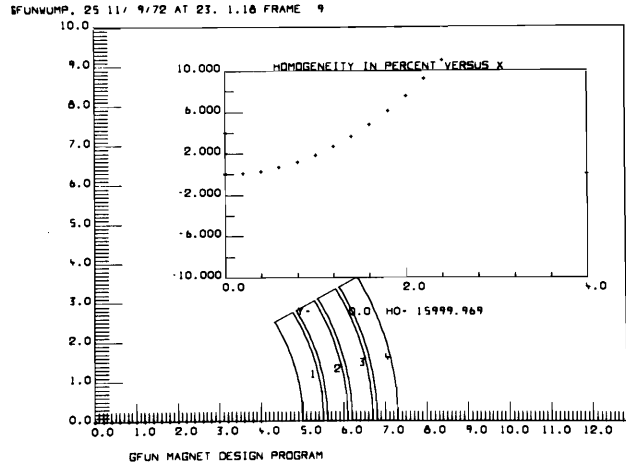


Fig. 2. Optimised dipole magnet. Initial current geometry and field homogeneity.

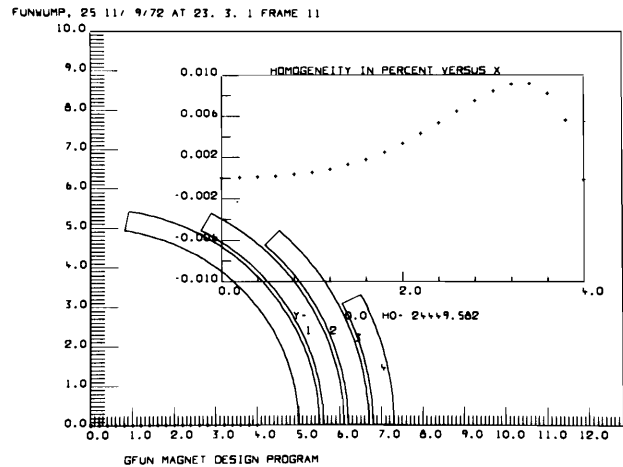


Fig. 3. Optimised dipole magnet. Optimisation without iron.

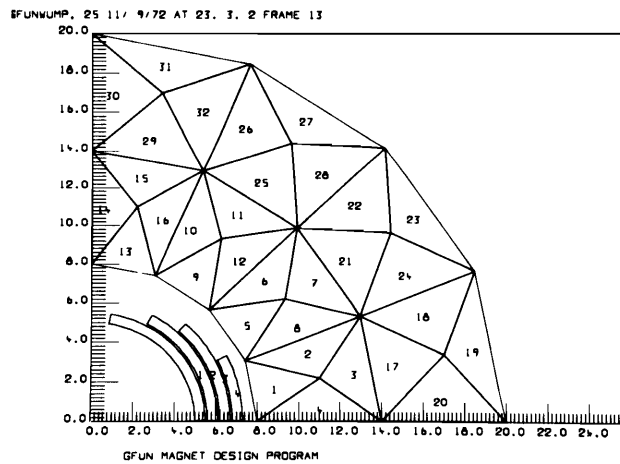


Fig. 4. Optimised dipole magnet. Geometry of cylindrical iron shield.

ICHI USED IS CHI CALCULATED

1 ITERATIONS. ELEMENT	1	CHANGED BY	289.51978
2 ITERATIONS. ELEMENT	9	CHANGED BY	85.59912
3 ITERATIONS. ELEMENT	9	CHANGED BY	104.50662
4 ITERATIONS. ELEMENT	13	CHANGED BY	132.62354
5 ITERATIONS. ELEMENT	13	CHANGED BY	186.29555
6 ITERATIONS. ELEMENT	13	CHANGED BY	203.60371
7 ITERATIONS. ELEMENT	13	CHANGED BY	242.81201
8 ITERATIONS. ELEMENT	13	CHANGED BY	279.61328
9 ITERATIONS. ELEMENT	13	CHANGED BY	309.54688
10 ITERATIONS. ELEMENT	13	CHANGED BY	328.01177
11 ITERATIONS. ELEMENT	13	CHANGED BY	331.65522
12 ITERATIONS. ELEMENT	13	CHANGED BY	320.47510
13 ITERATIONS. ELEMENT	13	CHANGED BY	296.00171
14 ITERATIONS. ELEMENT	13	CHANGED BY	227.62988
15 ITERATIONS. ELEMENT	9	CHANGED BY	188.42095
16 ITERATIONS. ELEMENT	9	CHANGED BY	125.22437
17 ITERATIONS. ELEMENT	9	CHANGED BY	71.34619
18 ITERATIONS. ELEMENT	5	CHANGED BY	52.90479
19 ITERATIONS. ELEMENT	5	CHANGED BY	44.40283
20 ITERATIONS. ELEMENT	5	CHANGED BY	37.00537
21 ITERATIONS. ELEMENT	5	CHANGED BY	30.78101
22 ITERATIONS. ELEMENT	5	CHANGED BY	25.64209
23 ITERATIONS. ELEMENT	5	CHANGED BY	21.44116
24 ITERATIONS. ELEMENT	5	CHANGED BY	18.00654
25 ITERATIONS. ELEMENT	5	CHANGED BY	15.19725
26 ITERATIONS. ELEMENT	5	CHANGED BY	12.86037
27 ITERATIONS. ELEMENT	5	CHANGED BY	10.96606
28 ITERATIONS. ELEMENT	5	CHANGED BY	9.37573
29 ITERATIONS. ELEMENT	5	CHANGED BY	8.04565
30 ITERATIONS. ELEMENT	4	CHANGED BY	6.92578
31 ITERATIONS. ELEMENT	4	CHANGED BY	6.21948
32 ITERATIONS. ELEMENT	4	CHANGED BY	5.91670
33 ITERATIONS. ELEMENT	4	CHANGED BY	5.62666
34 ITERATIONS. ELEMENT	4	CHANGED BY	5.34839
35 ITERATIONS. ELEMENT	4	CHANGED BY	5.07784
36 ITERATIONS. ELEMENT	4	CHANGED BY	4.81783
37 ITERATIONS. ELEMENT	4	CHANGED BY	4.56738

Fig. 5. Optimised dipole magnet. Convergence of the field in the iron.

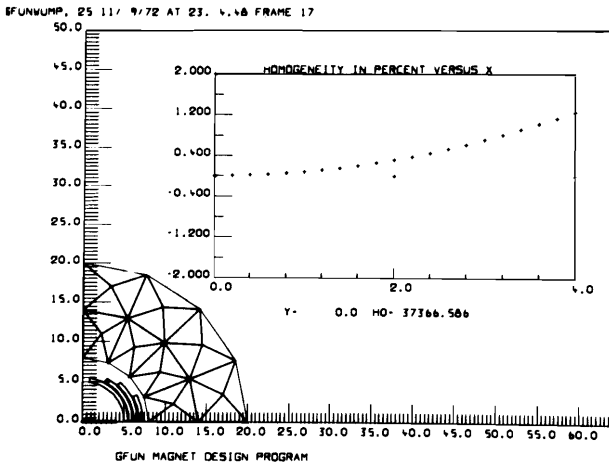


Fig. 6. Optimised dipole magnet. Homogeneity of combined fields from current and iron.

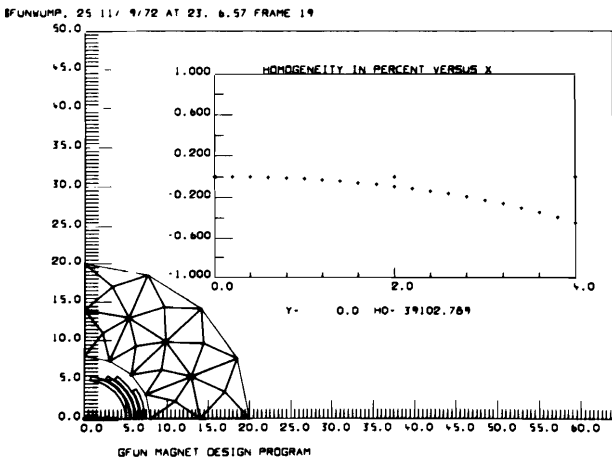


Fig. 7. Optimised dipole magnet. Homogeneity after one re-optimisation.

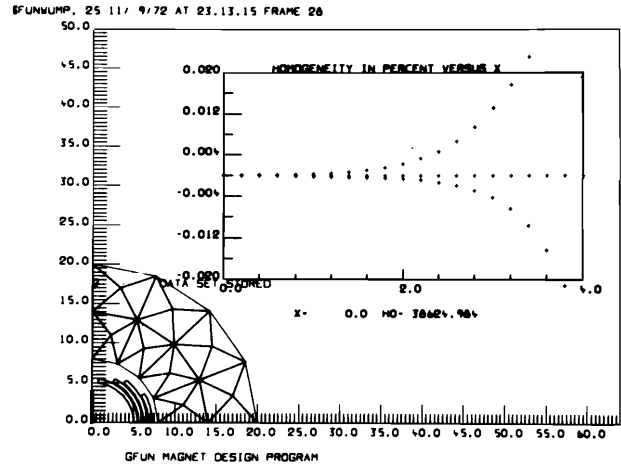


Fig. 8. Optimised dipole magnet. Homogeneity after several optimisation cycles.

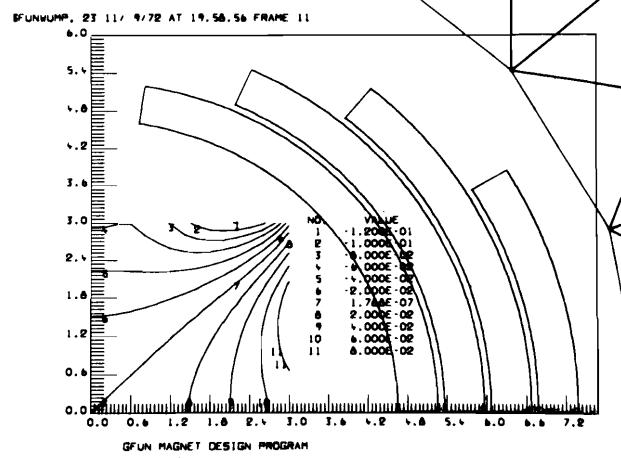


Fig. 9. Optimised dipole magnet. Homogeneity contours.

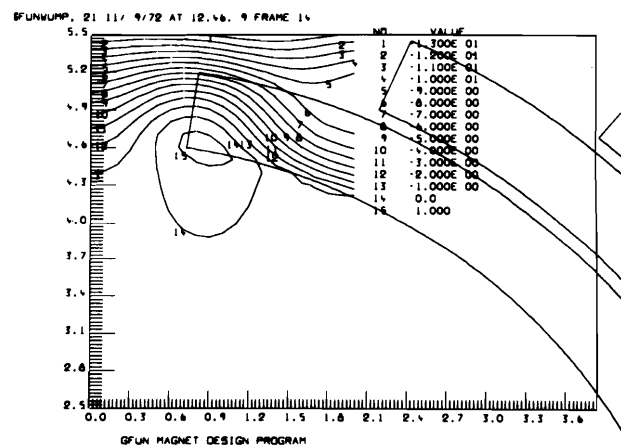


Fig. 10. Optimised dipole magnet. Contours showing peak field in windings.

The fifth point results in an addition to the graphics capabilities of GFUN. In trying to present all geometrical information about a three-dimensional structure of elements, one view is insufficient, and two or three orthogonal views are not immediately interpretable, and may be misleading for complicated designs. A rotated projection or a perspective view presents well-known difficulties. If hidden lines are shown, the picture is confusing at best and ambiguous at worst. If they are not shown, all information is not included, and some errors will not be detected.

We decided to produce stereoscopic views on the screen and attach a stereo viewer for viewing them. That way the user has all the geometrical information at one glance. The STEREO subprograms enable the designer to look at any number of iron elements he chooses and to view them from any angle. Stereo views of the iron for two magnets appear in Fig. 11, and 14. Presumably the reader who has consulted Morse and Feshbach<sup>11</sup> has come to terms with his ability or inability to view stereo pairs on a printed page; viewing bright lines against the dark screen with a suitable viewer is much easier.

### VII. Results

The two dimensional version of the program has been used extensively in the design of many magnets including polarised target magnets, inflector magnets, separator magnets, superconducting dipoles, and others. Because of space limitations details of these results will not be included in this paper. However, some results of calculations on a polarised target magnet and a superconducting dipole appear in another paper published in these Proceedings.<sup>12</sup>

The following examples are given of the use of the three dimensional version of the program.

It has been proposed that the magnet of the Rutherford Laboratory helium bubble chamber be modified for use with a rapid-cycling hydrogen bubble chamber. The coil separation would be increased and the iron return path modified. As a preliminary step to the study of how these changes would affect the field, we have used GFUN to calculate the magnet as it exists and have computed the results with measurements of the field.

The magnet consists of a Helmholtz pair of 2 x 6 double pancake coils, two hexagonal pole plates, and six return legs. In the calculation, the field due to the coils was taken as axisymmetric, and by the symmetry of the design, only one octant of the iron was required. Each half return leg was divided into eight triangular prisms, a total of twelve in the octant. The quarter hexagonal pole plate with a circular hole was approximated by twelve triangular prisms filling an annular region. Figure 11 shows stereo views of one octant of the iron.

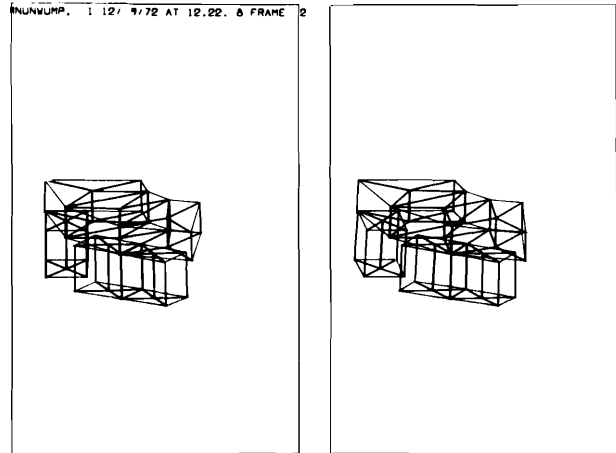


Fig.11. Helium bubble chamber magnet. Stereo views of one octant of iron.

Another calculation was performed in which the quarter pole plate was approximated by forty triangular prisms filling an annular region. The total number of iron elements was 52. See Fig.12. Figure 12 shows a projection of the iron on the x-y plane, and a plot of total field against radius.

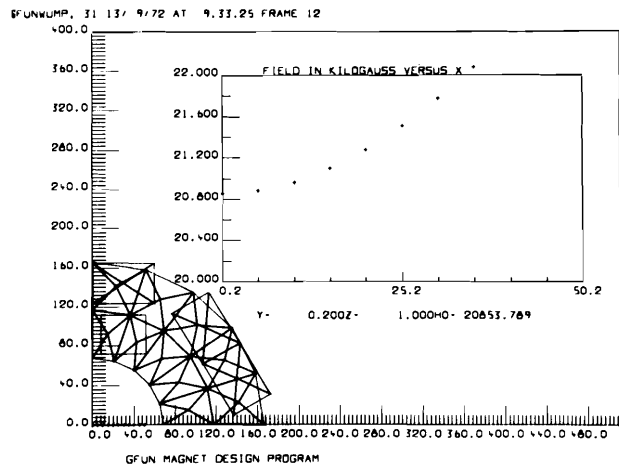


Fig.12. Helium bubble chamber. Radial variation of field in the median plane.

The field had been measured at the centre of the magnet and at points where the edges of the bubble chamber occur. The measured and calculated field at these points are compared in Table 1. The results with 24 iron elements and with 52 iron elements are much the same and are one per cent lower than the measured values. It should be noted that assuming axial symmetry, ie. replacing the return legs by an annular region as well, gave results that differed from the measured field by about 10 per cent.

TABLE I. Comparison of Measured and Calculated Fields for the RHEL Helium Bubble Chamber Magnet

Point cm	Measured kG	Calculated 52 element kG	Calculated Current only kG
(0, 0, 0)	20.95	20.86	14.83
(0, 0, 20.3)	19.82	19.97	14.41
(40.6, 20.3, 20.3)	22.52	22.49	15.67

A year ago, a calculation was performed with TRIM, assuming axial symmetry, to find the current needed to produce a central field of 23 kG. Although a GFUN calculation assuming axial symmetry disagreed with the measured field in the magnet, it might agree with the TRIM calculation which also assumed axial symmetry. So the same 36 element GFUN geometry shown in stereo view in Fig. 13 was rerun at the same higher current used in the TRIM calculation. The TRIM calculation yielded a central field of 23.00 kG; GFUN gave a 22.88 kG.

Comparison of the respective GFUN calculations with the actual measurements and with the TRIM calculations suggests that GFUN promises to be useful in three-dimensional field calculations.

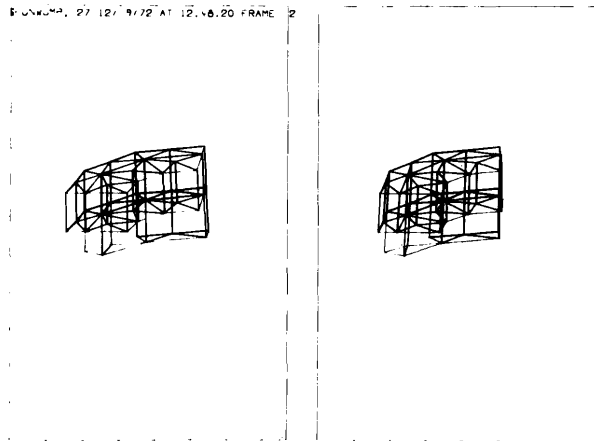


Fig.13. Helium bubble chamber. Stereo views of axi-symmetric model.

C Magnet

Extensive modifications of a C Magnet at the Rutherford Laboratory have spawned several TRIM calculations and some recent measurements. An attempt has been made to calculate this C Magnet with the three-dimensional version of GFUN but GFUN is at present inadequate in two ways. First the pole tips are tapered; but as GFUN accepts only prismatic elements, the calculations must use

stepped pole tips. Second the yoke of the magnet is mild steel and the pole tips are made of 38% Cobalt iron, but GFUN accommodates at present a single B-H curve for all iron elements.

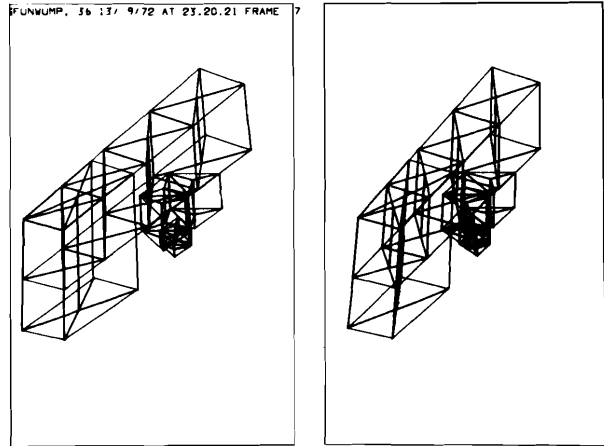


Fig.14. C Magnet. Stereo views of one quadrant of iron.

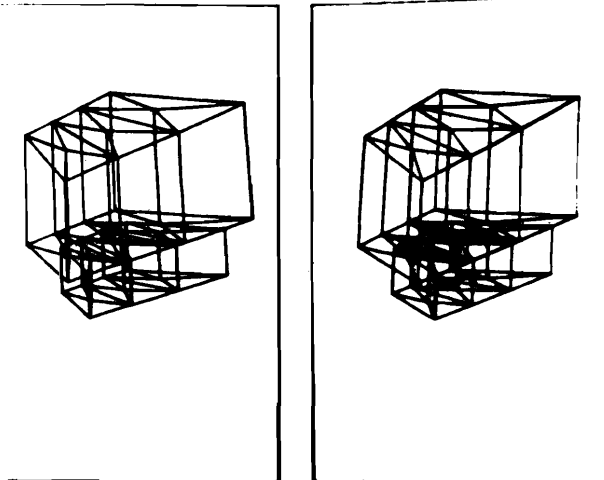


Fig.15. C Magnet. Stereo views of step approximation used for tapered pole tip.

As it is a C Magnet, there are only two symmetry planes and a full quadrant of the iron must be calculated. The field due to the coils is axisymmetric. A quadrant of the iron is shown in stereo in Fig. 14. A quadrant of the C is made up of 16 triangular prisms. The half pole piece is approximated by two half-hexagonal solids, each divided into 12 triangular prisms, there are a total of 40 iron elements, Figure 15 gives a stereo view of the half pole piece. Figure 16 shows an x-y projection of the pole piece and a z-r projection of the current elements.

Two calculations were performed. In the first the entire iron structure was assumed made of mild steel; in the second it was assumed to be 38% Cobalt iron. A curve of the variation of total field against radius in the midplane shown for one calculation in Fig. 17.

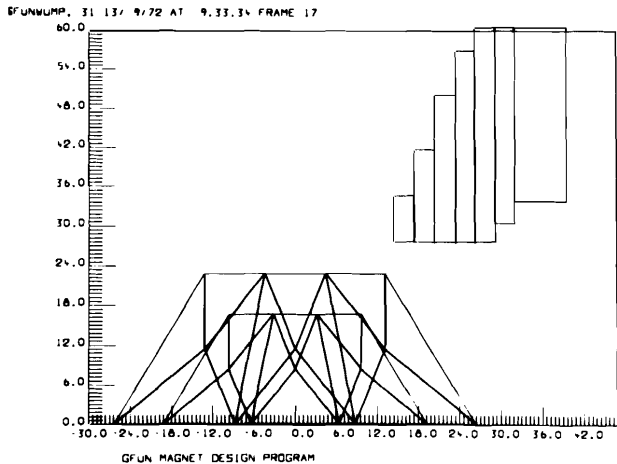


Fig.16. C Magnet. X-Y projection of the pole tip, Z-R projection of current elements.

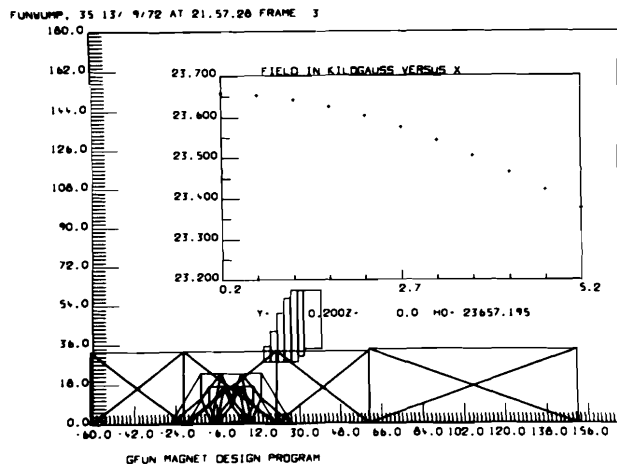


Fig.17. C Magnet. Radial variation of field.

The measured central field is 25.00 kG; the field calculated assuming all mild steel is 20.28 kG; and the field calculated assuming 38% Cobalt iron is 23.66 kG. The agreements are not as good as with the helium bubble chamber magnet, probably because of the inadequacies described above.

#### VIII. Conclusions

The two-dimensional program represents three major advances on most existing programs, and the extension to three dimensions satisfies a long standing requirement.

The first advance is in the use of the direct method. The removal of the boundary condition problem; the ability to represent accurately small discontinuities in the conductors; and the abolition of elements in the air regions are valuable features.

The second advantage is in the use of interactive graphics. Data preparation is reduced to a minimum and immediate visual checks are available. Without these facilities the three-dimensional problem would be especially tedious. Graphs can be plotted and contour maps drawn on the screen, and hard copies taken of final results. Design data and magnetisation data are stored on disk in a named file for subsequent interrogation or modification.

The third advance is in the use of optimisation routines. Intelligent use of the automatic optimisation facilities by an experienced magnet designer makes efficient use of the man-machine combination. The ease with which different designs can be tried encourages designers to use their intuition.

Current effort is directed towards programming iron and current elements of general shape, towards expanding the automatic optimisation facilities, and towards improving the generality of the three dimensional current model.

#### IX. Acknowledgements

The authors are indebted to Dr D B Thomas for encouragement throughout this work. Thanks are also due to Mr J Simkin for providing routines for the Harmonic analysis, and to Dr D B Scott for providing the graphics package, and direct access filing system.

#### X. References

1. A M Winslow, J of Computational Physics 1, 2 (1966)
2. R Taylor, "Daedalus - 360 (User's Guide)", Rutherford Laboratory Memorandum RHEL/M110 (1966)
3. D B Scott, "An Interactive Graphical Package and Direct Access Filing System for Computek Displays", Rutherford Laboratory Memorandum RHEL/M/C14 (1971)
4. M J Newman, "A Message Decoding System for use with the Interactive Graphics Package LDMPX", Rutherford Laboratory Memorandum RHEL/M/A19 (1972).
5. A A Halacsy, Proc. 2nd Reno Conf. on Analysis of Magnetic Fields, Nevada (1969), p.56
6. S Sackett, Proc. 2nd Reno Conf. on Analysis of Magnetic Fields, Nevada (1969), p.67
7. S Zaky, Proc. 3rd Reno Conf. on Magnetic Field Fields, Nevada (1971), p.142
8. S Robertson, Proc. 3rd Reno Conf. on Magnetic Fields, Nevada (1971), p.159
9. R A Beth, J. Appl. Phys. 37, 2568 (1966)
10. M J D Powell, Computer Jour. 7, 155 (1964)



11. P M Morse & H Feshbach, Methods of Theoretical Physics. (McGraw Hill, NY. 1953), Vol. 1, p. viii.
12. C W Trowbridge, Proc. 4th Int. Conf. on Magnet Technology, Brookhaven (1972)
13. T D Peel, D Roaf, et al. Proc. 2nd Int.Symp. Magnet Technology, Oxford, 1967, p.722

Appendix: The C Coefficients

Two-Dimensional Calculations

Equation (4) is a vector equation: both  $H$  and  $M_0$  are two component vectors, and  $C_{k\ell}^{mk}$  the coefficient between element  $\ell$  and field point  $k$  is a two by two tensor. If we let  $r = [(x_k - x_\ell)^2 + (y_k - y_\ell)^2]^{\frac{1}{2}}$ , and  $A_\ell$  be the area at element  $\ell$ , then the  $C_{k\ell}$  can be written as:

$$C_{kx, x\ell} = \frac{1}{2\pi} \iint_{A_\ell} \frac{[(x_k - x_\ell)^2 - (y_k - y_\ell)^2]}{r^4} dx_\ell dy_\ell \quad (A1a)$$

$$C_{ky, y\ell} = \frac{1}{2\pi} \iint_{A_\ell} \frac{2(x_k - x_\ell)(y_k - y_\ell)}{r^4} dx_\ell dy_\ell \quad (A1b)$$

$$C_{ky, x\ell} = C_{kx, y\ell} \quad (A1c)$$

$$C_{kx, y\ell} = -C_{kx, x\ell}$$

if point  $k$  is outside element  $\ell$  (A1d)

$$C_{ky, y\ell} = -1 - C_{kx, x\ell}$$

if point  $k$  is inside element  $\ell$  (A1e)

If the magnet has one or more planes of symmetry, the Eq (A1) are evaluated for the direct element and for each reflected element; the coefficients are added or subtracted depending on the symmetry. Eq.(A1c)-(A1e) will hold for each direct or reflected element separately; but because the two components may be added or subtracted differently they will not hold in general for the net coefficients.

Equation (A1) can be solved analytically if the element  $\ell$  is a polygon of  $n$  sides. Let us simplify our notation by writing

$$x_k = x_0, \quad y_k = y_0, \quad x_\ell = x, \quad y_\ell = y.$$

Let us use the subscript  $j$  to denote the vertex of the polygon, taken in anti-clockwise order. Then Eq (A1a) and (A1b) yield:

$$C_{kx, x\ell} = \frac{1}{2\pi} \sum_{j=1}^n (\sin^2 \phi_j - \sin^2 \phi_{j-1}) \tan^{-1} (y_j - y_0) / (x_j - x_0) + (\sin \phi_j \cos \phi_j - \sin \phi_{j-1} \cos \phi_{j-1}) \ln r_j \quad (A2a)$$

$$C_{kx, y\ell} = \frac{1}{2\pi} \sum_{j=1}^n (-\sin \phi_j \cos \phi_j + \sin \phi_{j-1} \cos \phi_{j-1}) \tan^{-1} (y_j - y_0) / (x_j - x_0) - (\cos^2 \phi_j - \cos^2 \phi_{j-1}) \ln r_j \quad (A2b)$$

$$\text{where } \phi_j = \tan^{-1} (y_{j+1} - y_j) / (x_{j+1} - x_j)$$

Care must be taken in evaluating Eq (A2) to use the correct value of the multi-valued arc-tangent function, especially in evaluating them when the field point is inside the element.

Eq (A2) can conveniently be written in terms of the complex variables  $z = x + iy$  and  $z_0 = x_0 + iy_0$ . If following Beth we let

$$\alpha_j = e^{-i\phi_j} \sin \phi_j$$

$$\text{and } G = \frac{1}{2\pi} \sum_{j=1}^n (\alpha_{j+1} - \alpha_j) \ln (z_j - z_0)$$

$$\text{then } C_{kx, x\ell} = \text{Re}(G) = -C_{ky, y\ell}$$

$$C_{kx, y\ell} = -\text{Im}(G) = C_{ky, x\ell}$$

where  $\text{Re}$  and  $\text{Im}$  denote respectively the real and imaginary parts.

Three-Dimensional Calculations

If in the steps leading up to Eq (4) we do not integrate over  $z$ , the same Eq (4) results; but now  $H$  and  $M_0$  are three-component vectors and  $C_{k\ell}$  is a three by three tensor. Let

$$r = [(x_k - x_\ell)^2 + (y_k - y_\ell)^2 + (z_k - z_\ell)^2]^{\frac{1}{2}}$$

and  $V_\ell$  be the volume of element. Then

$$C_{kx, x\ell} = \frac{1}{4\pi} \iiint_{V_\ell} \frac{[3(x_k - x_\ell)^2 - r^2]}{r^5} dx_\ell dy_\ell dz_\ell \quad (A6a)$$

$$C_{kx,ly} = \frac{1}{4\pi} \iiint_{V_\ell} \frac{3(x_k - x_\ell)(y_k - y_\ell)}{r^5} dx_\ell dy_\ell dz_\ell \quad (A6b)$$

with analogous expressions for the other seven components. The diagonal elements obey:

$$C_{kx,lx} + C_{ky,ly} + C_{kz,lz} = 0 \text{ if the field point } k \text{ is outside the element } \ell$$

$$= -1 \text{ if the field point } k \text{ is inside the element } \ell \quad (A7)$$

The Equations (A6) have been solved analytically for elements which are triangular or rectangular right prisms oriented in the z direction. Again let us adopt the notation

$$x_k = x_o, y_k = y_o, z_k = z_o, x_\ell = x, y_\ell = y, z_\ell = z$$

Let the subscript  $i=1, 2$  label the bottom and top faces of the prism and the subscripts  $j, m=1, 2, 3$  label the vertices and sides of each triangular face. Then if we introduce the expressions:

$$T_{ijm} = \tan^{-1} \frac{(z_i - z_o) [(y_j - y_o) \sin \phi_m + (x_j - x_o) \cos \phi_m]}{r_{ij} [(x_j - x_o) \sin \phi_m - (y_j - y_o) \cos \phi_m]} \quad (A8a)$$

$$L_{ij} = \frac{1}{2} \ln (r_{ij} + z_i - z_o) / (r_{ij} - z_i + z_o) \quad (A8b)$$

$$V_{ijm} = \frac{1}{2} \ln [(y_j - y_o) \sin \phi_m + (x_j - x_o) \cos \phi_m + r_{ij}] \quad (A8c)$$

we can write the coefficients:

$$C_{kx,lx} = \frac{1}{2\pi} \sum_{i=1}^2 (-1)^i \sum_{j=1}^3 \sin \phi_j [\sin \phi_j (T_{ijj} - T_{i,j+i,j}) - \cos \phi_j (L_{ij} - L_{i,j+1})] \quad (A9a)$$

$$C_{kx,ly} = \frac{1}{2\pi} \sum_{i=1}^2 (-1)^i \sum_{j=1}^3 \cos \phi_j [\cos \phi_j (T_{ijj} - T_{i,j+1,j}) + \sin \phi_j (L_{ij} - L_{i,j+1})] \quad (A9b)$$

$$C_{kx,ly} = \frac{1}{2\pi} \sum_{i=1}^2 (-1)^i \sum_{j=1}^3 \cos \phi_j [\sin \phi_j (T_{ijj} - T_{i,j+1,j}) + \cos \phi_j (L_{ij} - L_{i,j+1})] \quad (A9c)$$

$$C_{kx,lz} = \frac{1}{2\pi} \sum_{i=1}^2 (-1)^i \sum_{j=1}^3 -\sin \phi_j (U_{ijj} - U_{i,j+1,j}) \quad (A9d)$$

$$C_{ky,lz} = \frac{1}{2\pi} \sum_{i=1}^2 (-1)^i \sum_{j=1}^3 \cos \phi_j (U_{ijj} - U_{i,j+1,j}) \quad (A9e)$$

Also

$$C_{ky,lx} = C_{kx,ly}$$

$$C_{kz,lx} = C_{kx,lz}$$

$$C_{kz,ly} = C_{ky,lz}$$

$$C_{kz,lz} = -C_{kx,lx} - C_{kx,ly}$$

if the field point  $k$  lies outside the element  $\ell$

$$C_{kz,lz} = -1 - C_{kx,lx} - C_{ky,ly}$$

if the field point  $k$  lies inside the element  $\ell$